

Design of an Exoskeleton as a Finger-Joint Angular Sensor *

Yimesker Yihun, Md Shamim N. Rahman and Alba Perez-Gracia¹

Abstract—Estimation of joint angles for human joints is important for many applications in Bioengineering. Most of the existing angular joint sensors rely on the assumption of the knowledge of the type of motion and location of the joint. This paper presents a new design for the measurement of finger joint angular motion. The design presented here consists of an exoskeleton, designed to fit the finger motion, in which we can relate the angular displacement of its links to the change in orientation of the phalanx under consideration. Unlike other designs, the exoskeleton does not need any information about the actual anatomy and dimensions of the hand in order to provide with the angular information. The design is to be used in myoelectrical signal identification.

I. INTRODUCTION

Accurate hand pose tracking and finger joint measurements are important research topics in bioengineering fields for different applications; the design of exoskeleton and prosthetic devices and the implementation of control algorithms are a few of those. Almost all currently available prosthetics using EMG or sEMG sensors compute some threshold value for the corresponding finger joint positions [1]. In most cases, models are obtained with the smoothed sEMG data as input and the respective smoothed finger angle data as output. The dynamic model obtained allows the instantaneous control of the finger motions. For these and other reasons, to relate the surface EMG signals to the finger motion, and also for gesture recognition, researchers have been using data gloves and expensive infrared sensors [2]. These devices tend to be expensive and affected by noise; in the case of glove devices, the fitting greatly influences the measurement error [3]. In addition, the accuracy of the result depends on a faithful underlying hand model, which is a complex problem on its own [4]. This paper presents a novel approach to estimate the finger joint-angles that can be applied for modeling of surface electromyography (sEMG) signals.

The approach presented here is based on creating an exoskeleton device, which can be attached to the hand, that links in a one-to-one relation the angular pose of the phalanx under consideration to the relative angle between two links of the exoskeleton. This relative angle is easy to sense in an accurate and inexpensive fashion. The exoskeleton design follows the approach of [5] and [6].

In order to design the exoskeleton, a camera vision system is used to track the hand motion. Non-contact technologies

are mostly vision-based or use infrared or magnetic technologies. Most of the focus in single-camera tracking has been with detecting the region of interest (ROI) of the hand. Some research has attempted to create simplified hand models through markerless detection [7], [8]. Work has also been done using markers [8] and multi camera systems [9]. In this research we are using a marker-based detection technique to get information about the finger motion.

Using the vision information as an input, the kinematic synthesis of the mechanism is performed to obtain the exoskeleton-based joint angle sensor. After that, a sensitivity analysis is performed in order to decide the location of the sensor. The linkage analysis yields the angular relation between the sensed angle and the limb orientation.

II. FINGER EXOSKELETON DESIGN

It is important to notice that the internal structure of the hand -the skeleton- is not a part of the exoskeleton mechanism. The mid phalanx of the finger is attached to the coupler of the linkage, as indicated in Figure 1, and the whole mechanism is placed on the dorsal carpal of the hand. The exoskeleton is designed for the coupler to follow a task motion -in this case, the motion of the phalanx. The exoskeleton mechanism is designed to be light and have a smooth motion over the range of the finger, so to minimize dynamic loading effects on the signal under study. An angular potentiometer is to be attached to one of the joints of the linkage, and the sensed angle is to be related to the angle of the coupler with respect to the fixed link.

Type synthesis, the selection of the topology of the mechanism to be used as exoskeleton, is a first step in the design process. For this sensor, the approach has been to try to use the simplest mechanism possible, for decreased complexity, weight and inertia on the finger. The planar four-bar mechanism was tried first, but it was not successful due to the interference of the links with the finger and the dorsal part of the hand in all designs. The six-bar linkage is the next simplest one. It allows positioning the links away from the finger so that no interference appears, while matching the planar 1-dof motion of the single finger joint. Thus, a planar, single-dof six-bar linkage (see Figure 6) has been selected as the exoskeleton topology.

III. FINGER INPUT DATA

The experimental approach to get the data is based on the principle that the pose of a calibrated camera can be uniquely determined from a minimum of four coplanar but non-collinear points. Thus, two squares attached to the proximal phalanges and to the dorsal part of the carpal are used as

*This work was supported by the US Department of the Army, award number W81XWH-10-1-0128 awarded and administered by the U.S. Army Medical Research Acquisition Activity. The content is solely the responsibility of the authors.

¹Dept. of Mechanical Engineering, Idaho State University, Pocatello, ID, USA. yihuyime@isu.edu, rahmmd2@isu.edu, perealba@isu.edu

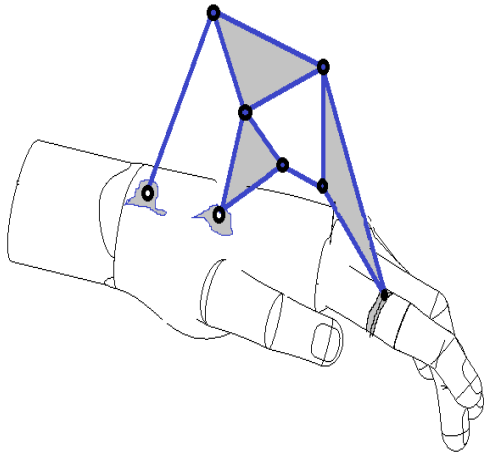


Fig. 1. Schematic drawing of the exoskeleton on the index finger

shown in Figure 3. Then the index finger is moved to its different positions/reaches. While moving the index finger, different frames are captured using a Dragonfly 2 camera from GreyPoint, with a Fujinon 1:1.4/9mm lens, interfaced with a computer using LabVIEW. The LabVIEW program captures and saves multiple images into the hard disk [10]. Once the frames are saved, sample frames from different orientation of the index finger are selected for processing.

In order to compute pose for 3D to 2D correspondences of a planar target, the algorithm used is based on Hager and Schweighofer [11]. The algorithm is customized to obtain a set of task positions from a video stream of a hand moving with markers. As it is clearly visible on the figure, the square on the dorsal carpal is used as a reference position, as the relative position between this square and the fixed joint of the mechanism is always constant while the index finger is moving.

The markers are used to estimate the pose, which consists of the position and orientation of the finger. An important aspect of this setup is the geometry of the markers. The geometry of a marker affects directly its performance and usability in computer vision applications. The design used by this project is a simple white square with a smaller black square inside as shown in Figure 3. It gives four sharp visible corners that form a perfect square to be used to find the 3D pose of the marker. Figure 5 shows a properly detected marker. It is important for these markers to be completely rigid for accurate pose estimation. For detection of the candidate points the Harris corner and edge detector algorithm [12] is used. To get a better result in both the detection and pose recovery, image segmentation is also performed so that the square corners are visible enough to be detected as shown in Figure 5. The overall methodology to design the exoskeleton-based sensor is shown in Figure 2.

The 3D pose recovery algorithm can map 3D reference points from the 2D image coordinates. It takes a set of non-collinear 3D coordinates of reference points $P_i = (x_i, y_i, z_i)^t, i = 1, \dots, n, n \geq 3$. These points can be expressed in an object-centered reference frame. The corresponding

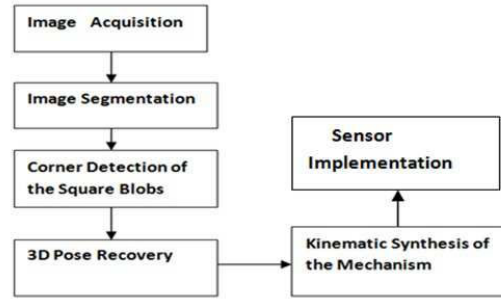


Fig. 2. The methodology adopted to design the exoskeleton based position sensor



Fig. 3. The captured image of the index finger with the square blobs on it

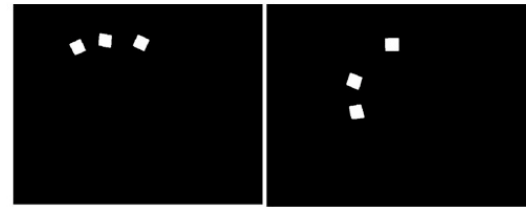


Fig. 4. The index finger movement and the square blobs

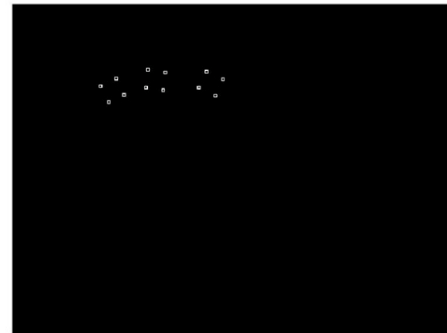


Fig. 5. Corner detection of one frame done by Harris corner detection

camera-space coordinates are $q_i = (x'_i, y'_i, z'_i)^t$. These two points are related by the rigid transformation

$$q_i = RP_i + t, \quad (1)$$

where R and t are the rotation matrix and translation vector respectively. Using this approach we obtain a transformation matrix T_{pi} for each position of the target point (the point from the square at the proximal phalanx) with respect to the camera and we also obtained T_{ci} (the point from the square at the carpal) with respect to the camera. In order to reference locally all movements of the target point, we use coordinate

transformation as $T_{cp} = T_{ci}^{-1}T_{pi}$. After getting T_{cp} , the transformation from the reference frame at the carpal to the proximal phalange, the design equations are formulated based on the candidate mechanism .

IV. EXOSKELETON DESIGN EQUATIONS

For this application, the desired mechanism is required to do two things: firstly, it should follow the trajectories described by the collected data; and secondly, there should be a one-to-one correspondence between the orientation of the MIP joint of the finger to one of the joints of the mechanism.

The six-bar linkage is the simplest closed, 1-dof planar linkage able to follow the collected trajectories accurately. On the other hand, being a simple, one-dof linkage, the relationships between all its angles and the driving joint angle are well known and can be related to the angle of the coupler and the MIP joint.

The variables defined for the six-bar mechanism are shown in Figure 6, where $\theta_1, \theta_2, \theta_3, \theta_4$ and θ_5 are the joint angles and the remaining parameters (i.e., $s_{1x}, s_{1y}, s_{4x}, s_{4y}, a, l_1, l_2, l_3, l_4, l_5, b_1, b_2, \alpha, \gamma$ and δ) are the structural variables of the mechanism. Compared with the more common four-bar mechanisms, six-bar mechanisms have more design variables, therefore with an appropriate design, six-bar mechanisms can adapt to a wider number of motions.

Using the variables defined in Figure 6, the forward kinematic equations for a planar six-bar mechanism are defined as [13], [14]

$$\begin{aligned}
& s_{1x} + l_1 \cos(\theta_1) + l_2 \cos(\theta_1 + \theta_2 + \gamma) + \\
& \quad a \cos(\theta_1 + \theta_2 + \gamma + \theta_3 + \alpha) - P_x = 0 \\
& s_{1y} + l_1 \sin(\theta_1) + l_2 \sin(\theta_1 + \theta_2 + \gamma) + \\
& \quad a \sin(\theta_1 + \theta_2 + \gamma + \theta_3 + \alpha) - P_y = 0 \\
& s_{1x} + l_1 \cos(\theta_1) + b_2 \cos(\theta_1 + \theta_2) - \\
& \quad (s_{4x} + b_2 \cos(\theta_4 + \delta)) = 0 \\
& s_{1y} + l_1 \sin(\theta_1) + b_2 \sin(\theta_1 + \theta_2) - \\
& \quad (s_{4y} + b_2 \sin(\theta_4 + \delta)) = 0 \\
& s_{1x} + l_1 \cos(\theta_1) + l_2 \cos(\theta_1 + \theta_2 + \gamma) + \\
& \quad l_3 \cos(\theta_1 + \theta_2 + \gamma + \theta_3) - (l_5 \cos(\theta_4 + \theta_5) + \\
& \quad l_4 \cos(\theta_4) + s_{4x}) = 0 \\
& s_{1y} + l_1 \sin(\theta_1) + l_2 \sin(\theta_1 + \theta_2 + \gamma) + \\
& \quad l_3 \sin(\theta_1 + \theta_2 + \gamma + \theta_3) - (l_5 \sin(\theta_4 + \theta_5) + \\
& \quad l_4 \sin(\theta_4) + s_{4y}) = 0. \tag{2}
\end{aligned}$$

From the set up we can also identify the following angular relation

$$\theta_1 + \theta_2 + \gamma + \theta_3 + \alpha + \beta - \varphi = 0. \tag{3}$$

The equations given above in (2) and (3) were used to determine the trajectory that point \mathbf{P} and its attached frame would follow through the operation of the mechanism. The axis shown in Figure 6 indicates the angle φ is the same as the one of the MIP joint of the finger.

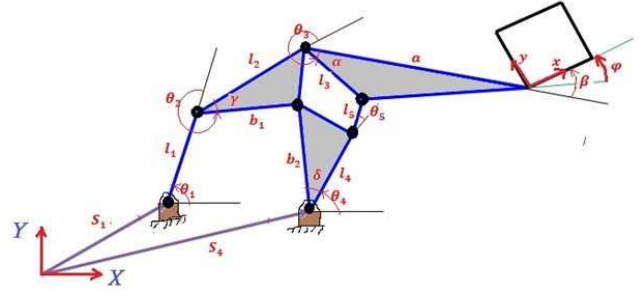


Fig. 6. The six-bar linkage with variables used

Nine positions are selected from the index finger trajectory. The end-effector location at the coupler link yields two equations, and the loop equations account for four equations for each position. This gives a total of 52 nonlinear equations. In addition, we have 9 angular equations; overall, we have 63 equations. The total variables to be found are 61 in total. Some auxiliary equations are added to limit the size of some key links in the linkage.

The equations are solved using a Levenberg-Marquardt nonlinear, unconstrained solver implemented in Java. This is based on public domain MINPACK routines, translated from FORTRAN to Java by Steve Verrill [15].

The process yields many solutions. Each solution took an average of 7.5 minutes on a 2.2GHz Intel Core i7. We solved several times, in groups of 50 runs, out of which approximately 3 solutions were acceptable each time. The acceptability was defined in terms of position on the hand, overall dimensions and hand interference. The accepted candidates were modeled using CAD software in order to select the final design.

V. ANGULAR MEASUREMENT

From the design of the mechanism it is shown that the angle φ corresponds to the orientation of the MIP joint of the finger. Thus, using (3) we can get the value of φ for every finite displacement of the finger in terms of the angles $\theta_1, \theta_2, \gamma, \theta_3, \alpha$ and β . Here α, γ and β are constants, and θ_1, θ_2 and θ_3 are the joint variables, which can be expressed in terms of one of them (for instance θ_1),

$$\varphi^i = \theta_1^i + \theta_2^i + \theta_3^i + \alpha + \beta + \gamma, \tag{4}$$

where i corresponds to any single measurement of the angle.

We use 4, together with the constraint relations between the joint angles [13] that give $\theta_2^i = f(\theta_1^i)$ and $\theta_3^i = f(\theta_1^i)$.

Therefore, the only variable that we need to measure is θ_1 . Since one of our objectives is to come up with a cost-effective sensing device, a resistive potentiometer is selected to be mounted on that joint of the six-bar mechanism to measure θ_1 . Similarly, relations can be found to place the sensor at any other joint.s

VI. SENSITIVITY ANALYSIS

The selection of the sensed angle is based on calculating the relative variation of each angle with respect to the MIP

joint angle φ . If possible, the sensor should be mounted on the joint that presents a higher sensitivity, defined as the ratio of change of the measured angle with respect to the change in the joint angle.

For this sensor, θ_1 has been selected as the sensed variable, due to the sensitivity analysis and also for accessibility in mounting and reading the sensor.

Figure 7 shows part of the motion in which a constant angular velocity of 1.5rad/sec is applied to joint1 θ_1 and the change of the angular position of each joint has been compared. From this figure we can deduce that all the other joint angles i.e. θ_2 , θ_3 and θ_4 have smaller angular changes than θ_1 and θ_5 . The angular velocity ratio has been calculated and it is shown in Figure 8 for the angle θ_1 . For mounting the potentiometer, we found that θ_1 is more convenient. The potentiometer is mounted as shown in Figure 9.

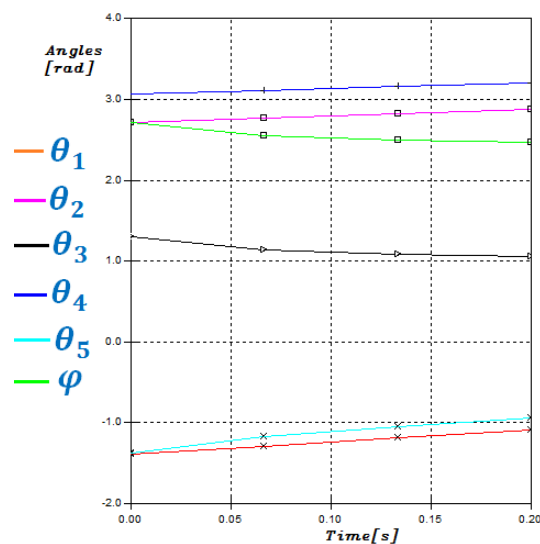


Fig. 7. The angular positions as a function of time

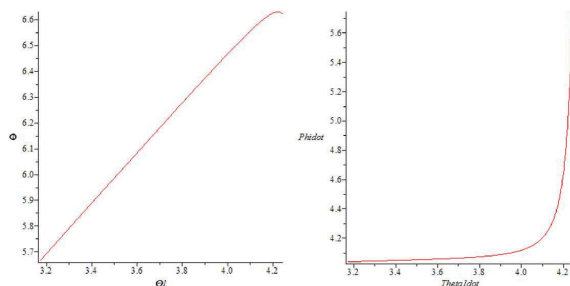


Fig. 8. Sensitivity analysis for θ_1

VII. RESULTS

The candidate designs were ranked considering size, mechanism placement and overall structure. The selected design is optimized and modeled as shown in Figure 10. The design parameters of the selected six-bar linkage are shown in Table I (angles in radians and lengths in millimeters).

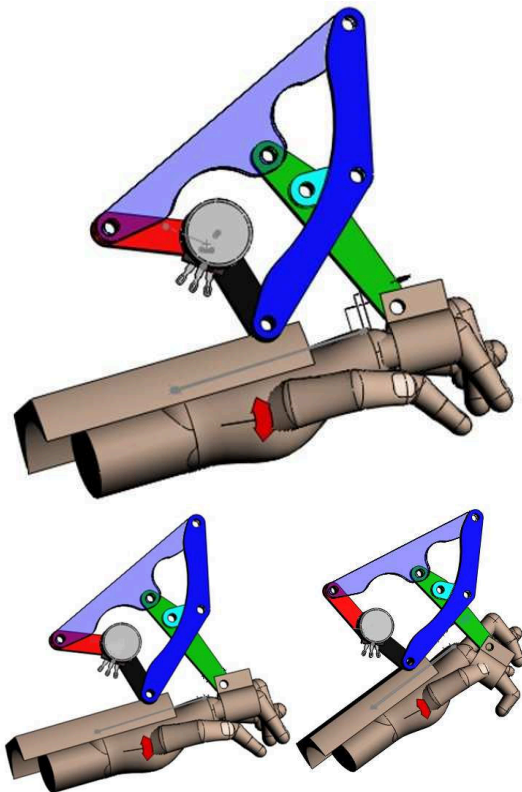


Fig. 9. The exoskeleton and the sensor on the hand, at two different configurations

TABLE I
EXOSKELETON DIMENSIONS

s_1	(46.34, -94.63)
s_4	(-30.49, -57.91)
a	-77.66
l_1	-40.01
l_2	-68.46
l_3	20.00
l_4	-68.46
l_5	20.00
b_1	-122.58
b_2	-122.57
γ	-0.27
α	3.04
δ	0.28
β	2.27

A rapid prototype has been built in order to further assess the performance of the sensor and it is shown in Figure 11. The final product will be made from aluminum and the estimated total cost for several joints, including machining, is within hundreds of dollars. We believe that this sensor will be cheaper than other sensors such as data gloves, magnetic, and infrared sensors, which cost in the order of thousands of dollars.

VIII. CONCLUSIONS

In this paper we present the development of a simple and cost-effective mechanism for the estimation of the angles of the Metacarpal interphalangeal (MIP) joint of the index

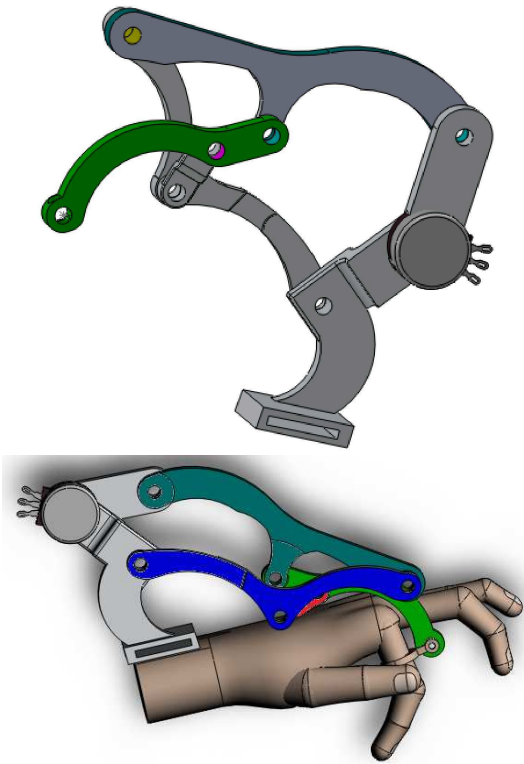


Fig. 10. CAD model of the selected linkage

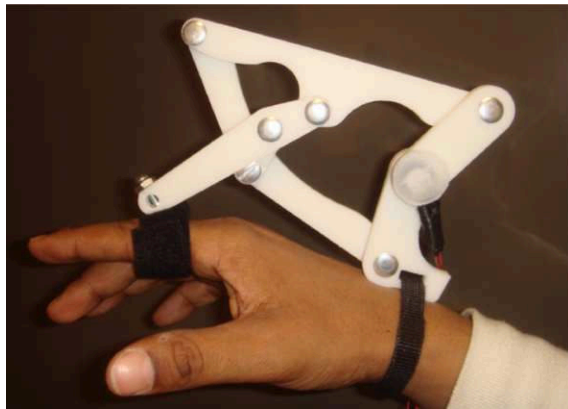


Fig. 11. Initial prototype of the selected linkage

finger. The design strategy includes vision system and image processing coupled with kinematic synthesis techniques.

The main advantage of this method is that it does not need any assumption about location and type of joints in the subject; the exoskeleton is going to follow the trajectory that is selected as task regardless of the skeleton structure that generates it. This allows for the creation of new and innovative exoskeleton-based position sensors which can help for EMG and position modeling in the grasp and control study. The application of image-processing techniques and use of a six-bar mechanism and a simple potentiometer grants a cheap, effective sensing device. The high number of solutions obtained means more choices for the designer

regarding placement and size of the exoskeleton.

Future research includes the dynamic analysis of the device and estimation of resolution, noise and possible loading effects on the sensed signal, as well as extension to other joints of the hand.

REFERENCES

- [1] P. K. Artemiadis and K. J. Kyriakopoulos, "Emg-based position and force control of a robot arm: Application to teleoperation and orthosis," in *int Conf. Rec. 2007 IEEE/ASME Int. Conf. on Advanced Intelligent Mechatronics, Zurich,*, October 10-13, 2004, 2007.
- [2] E. A. Matthias Rehm, Nikolaus Bee, "Wave like an egyptian - accelerometer based gesture recognition for culture specific interactions," in *British Computer Society*, 2007.
- [3] M. Kolsch and M. Turk, "Fast 2d hand tracking with flocks of features and multi-cue integration," in *Computer Vision and Pattern Recognition Workshop, May 27-June 2004*, 2004.
- [4] G. Stillfried and P. van der Smagt, "Movement model of a human hand based on magnetic resonance imaging (mri)," in *Proceedings of the 1st Int. Conf. on Applied Bionics and Biomechanics, Venice, Italy*, October 14-16., 2010.
- [5] D. Sands, A. Perez-Gracia, J. McCormack, and E. Wolbrecht, "Design method for a reconfigurable mechanisms for finger rehabilitation," in *Proceedings of the 2010 IASTED Robotics and Applications Conference*, November 1 3, 2010, Cambridge, Massachusetts, USA, 2010.
- [6] E. Wolbrecht, D. Reinkensmeyer, and A. Perez-Gracia, "Single degree-of-freedom exoskeleton mechanism design for finger rehabilitation," in *Proceedings of the ICORR 2011: Int. Conference on Rehabilitation Robotics*, June 29-July 1, 2011, Zurich, Switzerland, 2011.
- [7] Z. Hang, R. Qiuqi, and C. Houjin, "A new approach of hand tracking based on integrated optical low analyse," in *Signal processing (ICSP), 2010 IEEE 10th International Conference on*, Oct 2010, 2010, pp. 1194-1197.
- [8] A. A. Lasenby, "Motion capture with constrained inverse kinematics for real-time hand tracking," in *Communications, control and Signal processing (ISCCSP)*, 2010, pp. 1-5.
- [9] T. K., "Remarks on robust extraction of hand's silhouette for 3d hand motion capture system," in *Industrial Electronics, 2009 (IECON 09), Annual Conference of IEEE*, 2009, pp. 326-2331.
- [10] H. Ahsan, "3d computer vision system for hand joint motion calculation," Ph.D. dissertation, College of Engineering, Idaho State University, Pocatello, ID, USA, 2008.
- [11] G. Schweighofer and A. Pinz, "Robust pose estimation from a planar target," *IEEE Transactions on Pattern Analysis and Machine Intelligence*, pp. 2024-2030, 2006.
- [12] C. H. Stephens and M., "A combined corner and edge detector," in *the 4th Alvy Vision conference*, 1988, pp. 147-151.
- [13] J. M. McCarthy and G. Soh, *Geometric Design of Linkages*, 2nd ed. New York: Springer-Verlag, 2010.
- [14] C. W. Wampler, "Solving the kinematics of planar mechanisms," in *1998 ASME Design Engineering Technical Conferences, Sept 13-16, 1998*, Atlanta, Georgia, USA, 1998.
- [15] *Optimization java package*, 2000, program library long writeup W5013[Online]. Available <http://www1.fpl.fs.fed.us/optimization.html>.